ISSN 1070-3284, Russian Journal of Coordination Chemistry, 2024, Vol. 50, No. 2, pp. 106–112. © Pleiades Publishing, Ltd., 2024.

Syntheses, Crystal Structure, and Properties of Two New Coordination Polymers from a Triphenylamino-Based Ligand

Q. Cai[a], *, J. Su[a], W. B. Tang[a], and X. H. You[a]

[a] *Zhuhai Rundu Pharmaceutical Co., Ltd., Zhuhai, 519040 China*

**e-mail: cqtc@rdpharma.cn*

Received July 25, 2023; revised September 12, 2023; accepted November 20, 2023

Abstract—Two new coordination polymers, namely, $\{[CdCl_2(BIPAB)_2]\cdot H_2O\}_n$ (**I**) (BIPAB = 4-(bis(4-(1H-imidazol-1-yl)phenyl)amino)benzonitrile) and $\{[NiCl_2(HBIPABA)_2]\cdot 2H_2O\}_n$ (**II**) (HBIPABA = 4-(bis(4-(1H-imidazol-1-yl)phenyl)amino)benzoic acid), have been successfully synthesized by using a triphenylamino-based ligand BIPAB, as original reactant and characterized by single-crystal X-ray diffraction, elemental analysis, infrared spectroscopy, TG, and luminescence. X-ray single crystal diffraction analysis (CCDC nos. 2283736 and 2283737 for **I** and **II**, respectively) shows that both compounds **I** and **II** crystallize in monoclinic crystal system with space groups are $P2/c$ and $P2_1$, respectively. All of them exhibit one-dimensional (1D) ribbon coordination chain formula as $[MCl_2(L)_2]_n$. However, the 1D chains were packing into different three-dimensional (3D) supramolecular frameworks mainly due to the uncoordinated additional functional groups on the ligand. For compound **I**, the 1D chains cross arrange to form a 3D supermolecule framework, in which the nitrile grouping showed as guest molecule to be accommodated by Cd_2L_2 ring on adjacent 1D chains; for compound **II**, the 1D chains were connected by the hydrogen bonds between in situ formed carboxyl groups to formed a two-dimensional (2D) hydrogen bonding network, and the 2D networks were further interpenetrated to forms a 3D supermolecule framework. Compounds **I** and **II** showed a thermal stability up to 380 and 280°C, respectively. Moreover, compound **I** exhibits an intense blue emission centered at 490 nm upon excitation at 370 nm.

Keywords: coordination polymer, triphenylamino-based ligand, crystal structure, photoluminescent property

DOI: 10.1134/S1070328423601085

INTRODUCTION

The design and construction of coordination polymers (CPs) have attracted much attention mainly due to not only their intriguing structures but also their extensive potential applications in electronic devices [1, 2], sensing [3, 4], magnetism [5, 6], separation [7, 9], adsorption [10, 11], catalysis [12], and so on. New CPs could be easily obtained by regulating the internal (metal ions, organic, counter anions) and/or external factors (temperature, solvent, pH, concentration, and so on) that influence the assembly process of CPs. Among them, organic ligands undoubtedly play a key role in the construction of new CPs with desirable structures and properties. Triphenylamino-based ligands, which contain three terminal coordination groups, have been proven to be effective ligands for constructing various CPs [13–17]. Most of the reported triphenylamino-based ligands possess identical terminal groups (homotopic ligands), while those possessing different terminal groups (heterotopic ligands) remain relatively less explored [18–20].

Herein, a triphenylamino-based ligand, 4-(bis(4-(1H-imidazol-1-yl)phenyl)amino)benzonitrile (BIPAB), was selected mainly because (i) it contains two imidazolyl groups that have strong coordination ability towards many metal ions [21, 22]. In addition, the angle between two imidazolyl groups is approximately 120°, and such a motif is beneficial for the formation of various subunits, such as rings and cages [23, 24]. (ii) It contains a nitrile group, which has a weaker coordination ability but is easily hydrolysed into carboxyl groups. The combination of two types of groups with different functions in a uniq ligand may be beneficial for constructing CPs with definite subunits; for example, one group is used for constructing secondary building units (SBUs), while the other group connects the SBUs to a higher dimensional network via coordination bonds and/or weak interactions [25–27].

Herein, the hydrothermal synthesis and crystal structure of two new CPs from BIPAB are reported. Interestingly, the CPs showed similar coordination chain structures assembled from metal ions and imidazole groups but different supramolecular structures due to the different additional groups. The as-synthesized CP samples were well characterized by single-crystal X-ray diffraction, elemental analysis, and infrared spectroscopy. Additionally, the thermal stability and photoluminescent properties of the selected compounds were also investigated in detail. It is noted that only CP based on this ligand has been reported [28].

EXPERIMENTAL

Materials and measurements. The ligand BIPAB was purchased from Shanghai Kylpharm Co., Ltd. through its customized service. All the other chemicals were of analytical grade quality and were commercially obtained from Tianjin Damao Chemical Reagent Factory without further purification. Infrared (IR) spectroscopy was carried out on a Perkin-Elmer 17300 FT-IR spectrometer with KBr pellets in the 400–4000 cm^{-1} region. Elemental analysis (C, H, and N) was performed on a Perkin-Elmer 240C elemental analyser. Thermogravimetric analysis (TGA) experiments were recorded on a NETZSCH STA 449 C thermogravimetric analyser with a heating rate of 10°C/min under an air atmosphere. The luminescent spectrum was determined by using an Edinburgh FLS-900 spectrophotometer.

Synthesis of compound I. A mixture of BIPAB (43.4 mg, 0.1 mmol), $CdCl_2 \cdot 2.5H_2O$ (18.3 mg, 0.1 mmol), and deionized water (10 mL) was added into a PTFE liner and sonicated for 20 min. The mixture was sealed in a stainless-steel autoclave and then heated at 150°C for three days under autogenous pressure. After cooling to room temperature for 24 h, colorless block-shaped crystals were obtained by filtering. The crystals were washed with deionized water and dried in air (yield: 70% based on BIPAB).

For $C_{50}H_{36}N_{12}Cl_2Cd$

Anal. calcd., %	C, 60.77	H, 3.67	N, 17.01
Found, %	C, 60.89	H, 3.71	N, 16.93

IR (KBr pellet; ν, cm^{-1}): 3450 m, 2221 s, 1599 s, 1513 s, 1381 m, 1310 s, 1269 m, 1182 w, 1119 w, 1055 m, 965 m, 833 m, 738 m, 660 m, 566 m, 542 m.

Synthesis of compound II. A mixture of BIPAB (43.4 mg, 0.1 mmol), $NiCl_2 \cdot 6H_2O$ (23.8 mg, 0.1 mmol), dilute nitric acid (1 M, 0.1 mL) and deionized water (10 mL) was added into a PTFE liner and sonicated for 20 min. The mixture was sealed in a stainless-steel autoclave and then heated at 150°C for three days under autogenous pressure. After cooling to room temperature for 24 h, colorless block-shaped crystals were obtained by filtering. The crystals were washed with deionized water and dried in air (yield: 60% based on BIPAB).

For $C_{50}H_{42}N_{10}O_6Cl_2Ni$

Anal. calcd., %	C, 59.55	H, 4.20	N, 13.89
Found, %	C, 60.01	H, 4.31	N, 13.77

IR (KBr pellet; ν, cm^{-1}): 3345 m, 3133 m, 1672 s, 1599 s, 1522 s, 1396 m, 1300 s, 1278 m, 1187 w, 1123 w, 1064 m, 733 m, 656 m, 538 m, 1119 m, 1025 w, 990 w, 860 w, 789 w, 753 w, 704 w, 563 w.

X-ray crystallography. Single-crystal X-ray diffraction data collection for compounds **I** and **II** was performed on a Rigaku SuperNova Dual Atlas diffractometer with graphite-monochromated Mo and CuK_α radiation ($\lambda = 0.71073$ Å), respectively, at 298 K. Multiscan absorption correction was performed by the SADABS program [29]. Structural solution and refinement based on F^2 were performed with the SHELXS-2016 and SHELXL-2016 program packages [30], respectively. Anisotropic thermal parameters were used to refine all nonhydrogen atoms. The hydrogen atoms on the uncoordinated water molecule in compound **I** were not added but were included in the formula. The contributions of disordered solvent molecules in the micropores were removed by SQUEEZE [31]. The details of the crystal parameters, data collection, and refinement for the title compound are summarized in Table 1, and selected bond lengths and angles with their estimated standard deviations are given in Table 2.

Crystallographic data for **I** and **II** have been deposited with the Cambridge Crystallographic Data Centre (CCDC nos. 2283736 and 2283737 for **I** and **II**, respectively; www.ccdc.cam.ac.uk/data_request/cif).

RESULTS AND DISCUSSION

Single-crystal X-ray diffraction reveals that compound **I** crystallizes in the monoclinic system with the space group of $P2_1/c$. There is one Cd(II) with an occupancy of 1/2, one Cl$^-$ anion, one BIPAB ligand, and half of the uncoordinated water molecule in the asymmetric unit. Cd(II) is six-coordinate by four imidazolyl N atoms from four different BIPAB ligands and two Cl-anions, thereby forming a distorted octahedral coordination geometry, as shown in Fig. 1a. The Cd–N bond lengths range from 2.377(4) to 2.404(4) Å, and the Zn–Cl bond distance is 2.5900(10) Å (Table 2), all of which are comparable to those observed for other related Cd(II) CPs based on imidazole-based ligands [32, 33]. The BIPAB ligand acts as a bidentate ligand that binds to two Cd(II) ions with its two imidazole groups, and the nitrile group remains uncoordinated. The angle between two imidazolyl groups on the BIPAB ligand is 105.5°, and the coordination angle between two adjacent N atoms in the Cd(II) center is approximately 89°. Their angles are approximately complementary; thus, the combination of two BIPAB ligands and two Cd(II) ions gives rise to a distorted quadrangular M_2L_2 ring. The Cd···Cd distance is 14.498(4) Å in the ring. Such rings were interconnected by Cd(II) ions, resulting in a ribbon chain [34, 35] extending along the (1 1 0) or (–1 1 0) directions (Fig. 1b). These 1D chains are

Table 1. Crystallographic data and structure refinements for the compounds **I** and **II**

Parameter	Value	
	I	**II***
Empirical formula	$C_{50}H_{38}N_{12}OCl_2Cd$	$C_{50}H_{38}N_{10}O_4Cl_2Ni$
Formula weight	1006.256	972.51
Temperature, K	293 (2)	293 (2)
Wavelength, Å	0.71073	0.71073
Crystal system	Monoclinic	Monoclinic
Space group	$P2_1/c$	$P2_1$
a, Å	11.2016(7)	10.189(2)
b, Å	9.2047(5)	22.426(5)
c, Å	20.9685(15)	10.686(2)
α, deg	90	90
β, deg	90.516(6)	93.60(3)
γ, deg	90	90
V, Å^3	2161.9(2)	2436.9(9)
Z	2	2
ρ_{calcd}, mg m^{-3}	1.546	1.325
μ, mm^{-1}	0.685	0.562
F(000)	1023.5	1004.0
θ range for data collection, deg	3.88–50	3.632–50
Max, min transmission	0.947, 0.927	0.940, 0.930
Reflections collected	12232	8543
Unique reflections	3802	6739
Reflections with $I > 2\sigma(I)$	2955	5245
R_{int}	0.0874	0.0397
$R_1{}^a$, $wR_2{}^b$ ($I > 2\sigma(I)$)	0.0549/0.1256	0.0964/0.2635
$R_1{}^a$, $wR_2{}^b$ (all data)	0.0717/0.1427	0.1120/0.2883
Goodness of fit on F^2	1.046	1.039
$\Delta\rho_{max}$ and $\Delta\rho_{min}$, e Å^{-3}	1.29/–0.71	0.43/–0.88

[a] $R_1 = \Sigma||F_0| - |F_c||/\Sigma|F_0|$, [b] $wR_2 = \{\Sigma[w(F_0^2 - F_c^2)^2]/\Sigma(F_0^2)^2\}^{1/2}$.

* The refinement results were obtained from squeeze data.

arranged in parallel on the ab plane to give rise to a 2D layer. The packing of 2D layers along the c direction leads to a 3D supramolecular framework (Fig. 1c). Interestingly, the 1D chains in the adjacent 2D layer extend along different directions, as shown in Fig. 1d. Further analysis indicated that the M_2L_2 ring in the 1D chain accommodates two nitrile groups from two adjacent 1D chains with different directions. Such accommodation may favor both entropy and enthalpy, thus helping to stabilize the supramolecular framework.

When introducing dilute nitric acid to the reaction system and employing Ni(II) as a metal ion, crystals of compound **II** were generated. Compound **II** crystallizes in monoclinic space group $P2(1)$. The asymmetric unit contains one independent Ni(II) ion, two HBIPABA ligands from the in situ hydrolysis of the BIPAB ligand, one coordinated water molecule, and some uncoordinated molecules. The coordination environment of the Ni(II) ion is similar to that of Cd(II) in compound **I**. It was coordinated by four imidazolyl N atoms and two Cl-anions (Fig. 2a). The single crystal data and IR spectra indicate that the nitrile group is transferred into a carboxyl group. Such a transformation may be due to the presence of acid, which is beneficial for the hydrolysis of nitrile groups. For compound **I**, the lack of acidic or basic conditions may help to retain the nitrile group. The coordination mode of HBIPABA is also similar to that in com-

Table 2. Selected bond lengths (Å) and angles (deg) for the compounds **I** and **II***

Bond lengths	*d*, Å	Bond lengths	*d*, Å	Bond lengths	*d*, Å
		Compound **I**			
Cd(1)–Cl(1)$^{\#1}$	2.5900(10)	Cd(1)–Cl(1)	2.5900(10)	Cd(1)–N(6)$^{\#2}$	2.404(4)
Cd(1)–N(6)$^{\#3}$	2.404(4)	Cd(1)–N(4)$^{\#1}$	2.377(4)	Cd(1)–N(4)	2.377(4)
		Compound **II**			
Ni(1)–Cl(2)	2.353(9)	Ni(1)–N(6)	2.055(11)	Ni(1)–N(5)	2.095(10)
Ni(1)–N(10)$^{\#1}$	2.086(10)	Ni(1)–N(1)$^{\#1}$	2.11(8)	Ni(1)–Cl(1)	2.474(10)
Bond angles	ω, deg	Bond angles	ω, deg	Bond angles	ω, deg
		Compound **I**			
Cl(1)$^{\#1}$Cd(1)Cl(1)	180	N(6)$^{\#3}$Cd(1)N(6)$^{\#2}$	180	N(4)$^{\#1}$Cd(1)N(6)$^{\#3}$	90.65(12)
N(6)$^{\#2}$Cd(1)Cl(1)	90.23(9)	N(4)$^{\#1}$Cd(1)Cl(1)$^{\#1}$	88.75(9)	N(4)Cd(1)N(6)$^{\#2}$	90.65(12)
N(6)$^{\#2}$Cd(1)Cl(1)$^{\#1}$	89.77(9)	N(4)$^{\#1}$Cd(1)Cl(1)	91.25(9)	N(4)$^{\#1}$Cd(1)N(6)$^{\#2}$	89.35(12)
N(6)$^{\#3}$Cd(1)Cl(1)	89.77(9)	N(4)Cd(1)Cl(1)	88.75(9)	N(4)Cd(1)N(6)$^{\#3}$	89.35(12)
N(6)$^{\#3}$Cd(1)Cl(1)$^{\#1}$	90.23(9)	N(4)Cd(1)Cl(1)$^{\#1}$	91.25(9)	N(4)$^{\#1}$Cd(1)N(4)	180.0
		Compound **II**			
Cl(2)Ni(1)Cl(1)	178.5(3)	N(6)Ni(1)Cl(1)	88.1(4)	N(10)$^{\#1}$Ni(1)N(5)	177.8(4)
N(6)Ni(1)Cl(2)	93.3(3)	N(5)Ni(1)Cl(2)	97.5(3)	N(10)$^{\#1}$Ni(1)N(1)$^{\#1}$	92(2)
N(6)Ni(1)N(5)	90.2(4)	N(5)Ni(1)N(1)$^{\#1}$	90(3)	N(10)$^{\#1}$Ni(1)Cl(1)	96.3(3)
N(6)Ni(1)N(10)$^{\#1}$	87.7(4)	N(5)Ni(1)Cl(1)	83.0(3)	N(1)$^{\#1}$Ni(1)Cl(2)	85(3)
N(6)Ni(1)N(1)$^{\#1}$	178(3)	N(10)$^{\#1}$Ni(1)Cl(2)	83.2(3)	N(1)$^{\#1}$Ni(1)Cl(1)	94(3)

* Symmetry transformations used to generate equivalent atoms: $^{\#1}$ $1 - x, -y, -z$; $^{\#2}$ $1 + x, -1 + y, z$; $^{\#3}$ $-1 - x, 1 - y, -z$ for compound **I**; $^{\#1}$ $1 + x, y, 1 + z$; $^{\#2}$ $-1 + x, y, -1 + z$ for compound **II**.

pound **I**, where the two imidazolyl groups bind to two Ni(II) ions and the carboxyl group is uncoordinated. Due to the similar coordination modes of metal ions and organic ligands, a similar 1D coordination ribbon chain was also observed in compound **II**, as shown in Fig. 2b. The coordination angle of the two imidazolyl groups on the HBIPABA ligand in compound **II** is 110.33°, which is slightly higher than that in compound **I**. The angular angle between two coordinated N atoms is approximately 92°. The Ni···Ni separation in the M_2L_2 ring is 14.295(4), which is also just slightly smaller than the Cd···Cd separation in compound **I**. All the above results indicate that the coordination chains in compounds **I** and **II** are similar.

Significant differences between compounds **I** and **II** exist in their supramolecular structures, which are largely dependent on the additional uncoordinated group. In compound **II**, the uncoordinated carboxylate group has a strong ability to form a six-number hydrogen bonding ring, which connects the 1D ribbon chain into a 2D network (Fig. 2c). If the metal ion and HBIPABA ligand are considered four- and three-connected nodes, respectively, the 2D hydrogen bonding network can be seen as a (4·62)2(42·62·82) net topological view. Interestingly, the 2D layers were inclined to interpenetrate into the 3D supramolecular framework, as shown in Fig. 2d and 2e. The hydrogen bonding ring in one 2D layer goes through the M_2L_2 ring in the other 2D layer.

The PXRD patterns of the simulated and as-synthesized compounds **I** and **II** are shown in Fig. 3. It can be seen that the peaks of the as-synthesized one basically match well to the simulated one, indicating the high phase purity of these compounds. The difference in the relative intensity of the peaks in the simulated and as-synthesized spectra is due to the preferred orientation of the crystals. The thermal stability of compounds **I** and **II** was investigated by TGA from room temperature to 800°C in an air atmosphere at a rate of 10°C min^{-1}. As shown in Fig. 4, no obvious weight loss can be detected before 380°C in compound **I** (uncoordinated water molecules in **I** may be released in the dry process), meaning that the framework is stable up to 380°C. The framework begins to decompose after that temperature. For compound **II**, the first weight loss of 3.5% from room temperature to 120°C is attributable to the release of one guest water molecule (calc. of 3.6%) in the asymmetric unit. Then, it is stable up to 280°C and begins to decompose as the temperature further increases.

It is well known that CPs based on *d*10 metal ions generally show photoluminescent properties [36, 37].

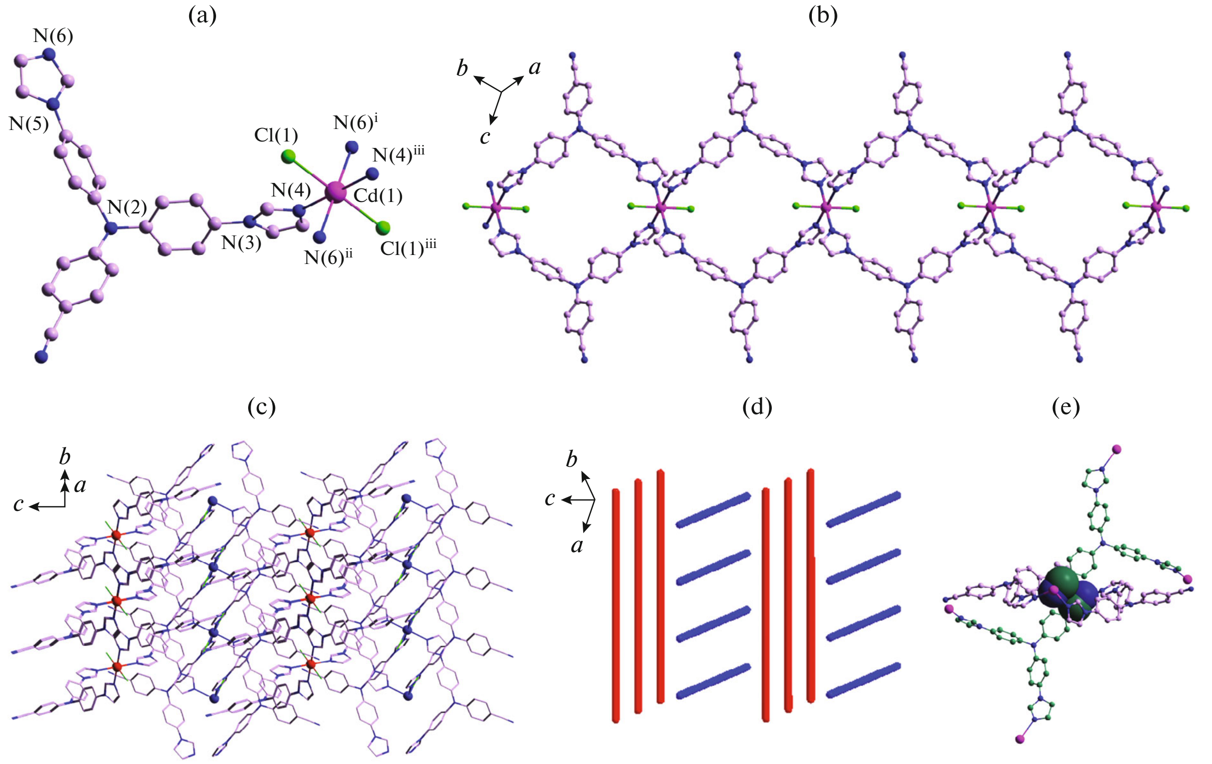

Fig. 1. The coordination environment of Cd(II) in compound **I** (a); the 1D ribbon chain in compound **I** (b); the 3D supramolecular framework in compound **I** (the Cd(II) ions in 1D chain with different directions are highlighted in red and blue (c); the arrangement of 1D chains in compound **I** (the 1D chains with different directions are highlighted in red and blue (d); the M_2L_2 ring in 1D chain are occupied by two nitrile groups from two adjacent chains in different directions (e).

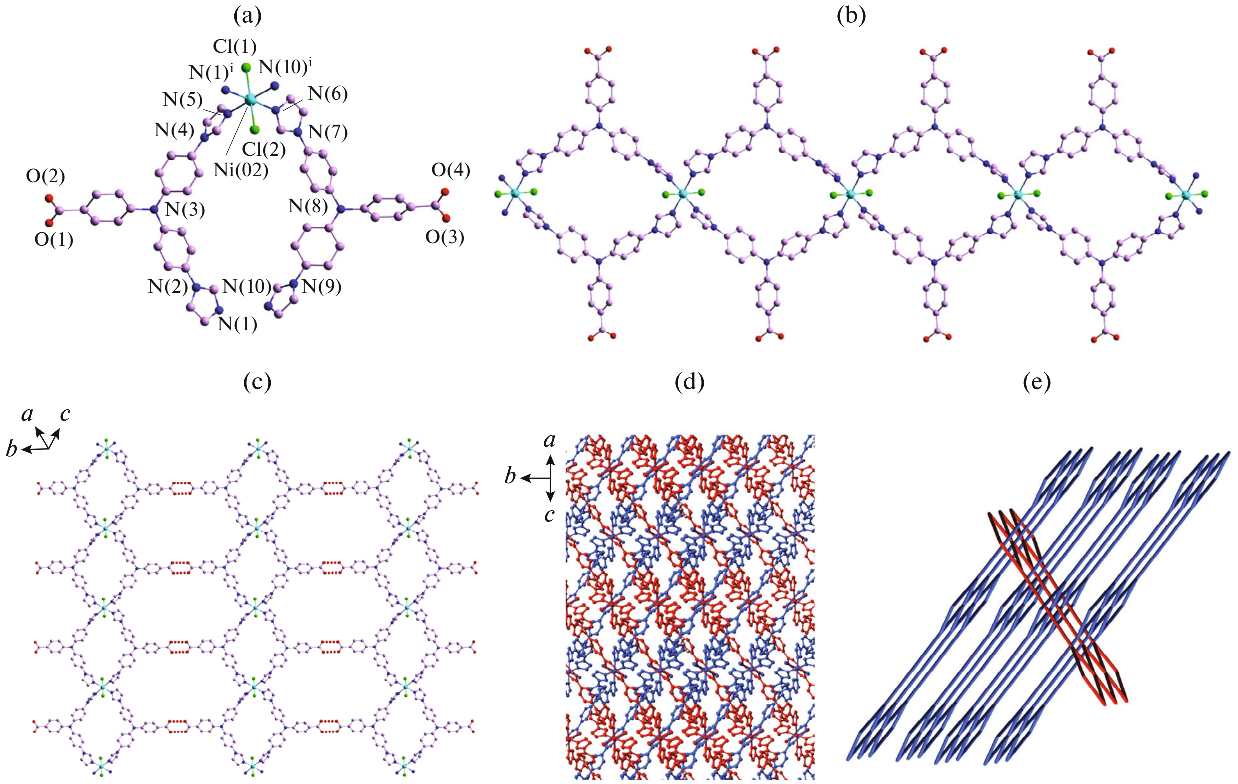

Fig. 2. The coordination environment of Ni(II) in compound **II** (a); the 1D ribbon chain in compound **II** (b); the 2D hydrogen bonding network in compound **II** (c); the 3D framework in compound **II** (the 2D nets with different directions are highlighted in red and blue) (d); the interpenetrated 2D networks in compound **II** (e).

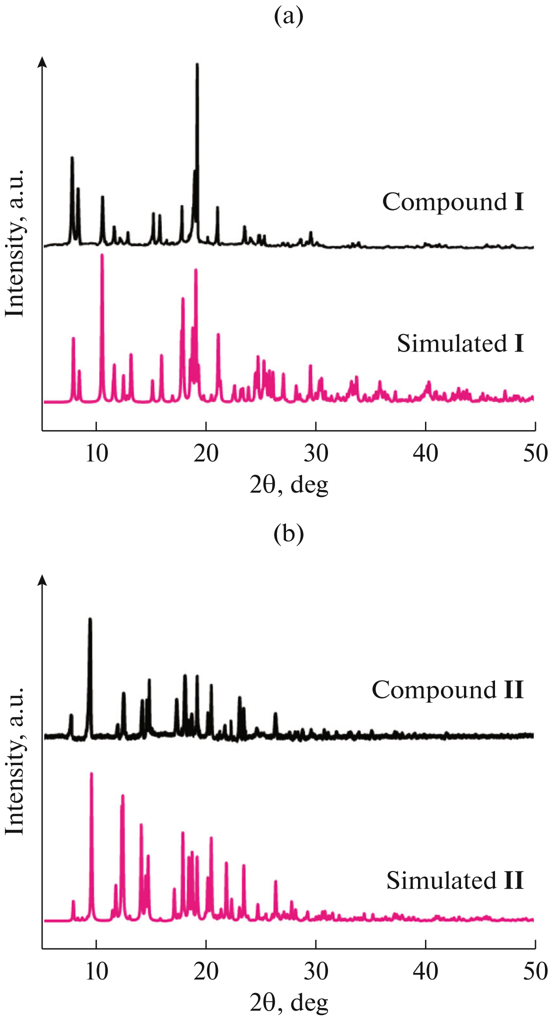

Fig. 3. The PXRD of simulated and as-synthesized compound I (a) and compound **II** (b).

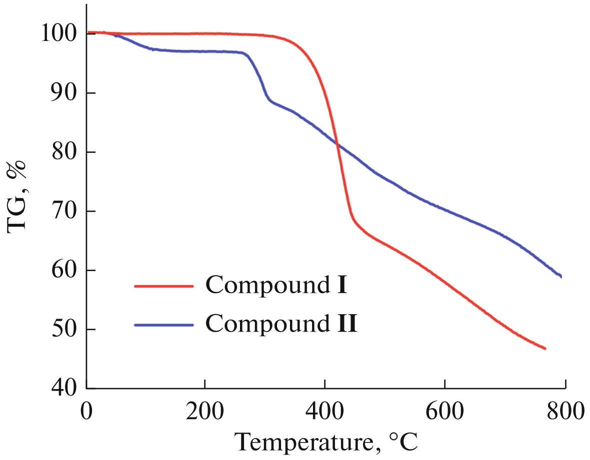

Fig. 4. TGA curves for compounds **I** and **II**.

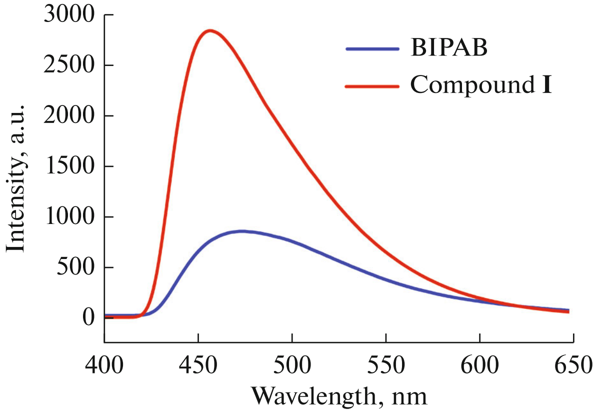

Fig. 5. Emission of BIPAB and compound **I** in the solid-state at room temperature.

Thus, the photoluminescent property of compound **I** was investigated. As shown in Fig. 5, compound **I** demonstrates strong blue luminescence with a maximum emission band at 453 nm when excited at 370 nm in the solid-state at room temperature. Compared with the BIPAB ligand, which showed an emission band centered at 458 nm when excited at 337 nm, compound **I** exhibited only a slight shift. Considering that the Cd(II) ion is difficult to oxidize or reduce, the emission of compound **I** may be attributed to intraligand transitions. The enhancement of the luminescence may be due to the coordination of Cd(II) ions to the BIPAB ligand, which fixes the conformation of the BIPAB ligand and reduces the nonradiative transition.

In conclusion, we successfully constructed and structurally characterized two new CPs synthesized from the same triphenylamino-based ligand. The nitrile group remained unchanged in compound **I**, whereas it was transferred into the carboxylate group in compound **II**. Compounds **I** and **II** display similar 1D ribbon coordination chains but with different supramolecular networks that are largely influenced by the additional uncoordinated functional group on the organic ligand. This work indicates that a triphenylamino-based ligand with two types of functional terminal groups is an effective organic ligand for the construction of new CP structures.

ACKNOWLEDGMENTS

We gratefully acknowledge the good suggestions of the structural solution by Dr. Zeller Matthias.

FUNDING

This work was supported by ongoing institutional funding. No additional grants to carry out or direct this particular research were obtained.

CONFLICT OF INTEREST

The authors of this work declare that they have no conflicts of interest.

REFERENCES

1. Zhang, L., Liu, H., Shi, W., and Cheng, P., *Coord. Chem. Rev.*, 2019, vol. 388, p. 293.
2. Zhang, K., Zeng, H.-Y., Wang, M.-X., et al., *J. Mater. Chem. A*, 2022, vol. 10, p. 11213.
3. Lu, K., Aung, T., Guo, N., et al., *Adv. Mater.*, 2018, vol. 30, p. e1707634.
4. Bhattacharjee, S., Bera, S., Das, R., et al., *ACS Appl. Mater. Interfaces*, 2022, vol. 14, p. 20907.
5. Zorlu, Y., Erbahar, D., Çetinkaya, A, et al., *Chem. Commun.*, 2019, vol. 55, p. 3053.
6. Yu, Q. and Wang, D., *J. Mater. Chem. A*, 2023, vol. 11, p. 5548.
7. Li, J.-R., Sculley, J., and Zhou, H.-C., *Chem. Rev.*, 2012, vol. 112, p. 869.
8. Karmakar, A., Samanta, P., Desai, A.V., et al., *Acc. Chem. Res.*, 2017, vol. 50, p. 2457.
9. Yang, L., Qian, S., Wang, X., et al., *Chem. Soc. Rev.*, 2020, vol. 49, p. 5359.
10. DeCoste, J.B. and Peterson, G.W., *Chem. Rev.*, 2014, vol. 114, p. 5695.
11. Mon, M., Bruno, R., Ferrando-Soria, J., et al., *J. Mater. Chem. A*, 2018, vol. 6, p. 4912.
12. Liu, J., Chen, L., Cui, H., et al., *Chem. Soc. Rev.*, 2014, vol. 43, p. 6011.
13. Hua, C., Baldansuren, A., Tuna, F., et al., *Inorg. Chem.*, 2016, vol. 55, p. 7270.
14. Zhuo, C., Wang, F., and Zhang, J., *Cryst. Growth Des.*, 2019, vol. 19, p. 3120.
15. Zhao, F.-J., Tan, Y.-X., Wang, W., et al., *Inorg. Chem.*, 2018, vol. 57, p. 13312.
16. Rizzuto, F.J., Faust, T.B., Chan, B., et al., *Chem. Eur. J.*, 2014, vol. 20, p. 17597.
17. Matikolaei, M.K. and Binaeian, E., *ACS Appl. Mater. Interfaces*, 2021, vol. 13, p. 27159.
18. Li, H., Wang, H., Gu, W., et al., *J. Fluoresc.*, 2023, vol. 33, p. 595.
19. Wang, G.-Q., Huang, J.-F., Huang, X.-F., et al., *Inorg. Chem. Front.*, 2021, vol. 8, p. 1083.
20. Wang, Y.X., Wang, H.M., Meng, P., et al., *Dalton Trans.*, 2021, vol. 50, p. 1740.
21. Xu, C., Luo, R., Zhang, D., et al., *J. Solid State Chem.*, 2021, vol. 303, p. 122535.
22. Qiu, Z.-F., Zhao, S.-M., Xu, Z.-H., et al., *Cryst. Growth Des.*, 2021, vol. 21, p. 5306.
23. Huang, J.F., Chen, Y.J., Liang, Z.H., et al., *Chin. J. Struct. Chem.*, 2022, vol. 41, p. 2202073.
24. Agarwal, R.A., Aijaz, A., Sanudo, C., et al., *Cryst. Growth Des.*, 2013, vol. 13, p. 1238.
25. Deng, S.Q., Mo, X.J., Zheng, S.R., et al., *Inorg. Chem.*, 2019, vol. 58, p. 2899.
26. Xian, J.Y., Yang, K., Wang, H.N., et al., *Inorg. Chem. Commun.*, 2021, vol. 130, p. 108720.
27. Huang, J.F., Hu, H.C., Deng, S.Q., et al., *New J. Chem.*, 2022, vol. 46, p. 7144.
28. Wang, G.Q., Huang, X.F., Wu, C.H., et al., *Polyhedron*, 2021, vol. 205, p. 115284.
29. Sheldrick, G.M., *SADABS, Program for X-Ray Crystal Structure Determination*, Göttingen: University of Göttingen, 1997.
30. Sheldrick, G.M., *Acta. Crystallogr., Sect C: Struct. Chem.*, 2015, vol. 71, p. 3.
31. Spek, A.L., *J. Appl. Crystallogr.*, 2003, vol. 36, p. 7.
32. Béziau, A., Baudron, S.A., and Pogozhev, D., *Chem. Commun.*, 2012, vol. 48, p. 10313.
33. Dey, A., Bairagi, D., and Biradha, K., *Cryst. Growth Des.*, 2017, vol. 17, p. 3885.
34. Petrosyants, S.P., Ilyukhin, A.B., and Sukhorukov, A., *Russ. J. Coord. Chem.*, 2005, vol. 31, p. 545. https://doi.org/10.1007/s11173-005-0134-y
35. Rossetti, A., Lippi, M., Martí-Rujas, J., et al., *Chem. Eur. J.*, 2018, vol. 24, p. 19368.
36. Xie, W., Wu, J., and Hang, X., *Front. Chem.*, 2021, vol. 9, p. 708314.
37. Chandra, A., Halder, S., Bhunia, S., et al., *J. Mol. Struct.*, 2023, vol. 1275, p. 34559.